

# Language-Grounded Dynamic Scene Graphs for Interactive Object Search with Mobile Manipulation

Daniel Honerkamp<sup>1\*</sup>, Martin Büchner<sup>1\*</sup>, Fabien Despinoy<sup>2</sup>, Tim Welschehold<sup>1</sup>, Abhinav Valada<sup>1</sup>

**Abstract**—To fully leverage the capabilities of mobile manipulation robots, it is imperative that they are able to autonomously execute long-horizon tasks in large unexplored environments. While large language models (LLMs) have shown emergent reasoning skills on arbitrary tasks, existing work primarily concentrates on explored environments, typically focusing on either navigation or manipulation tasks in isolation. In this work, we propose MoMa-LLM, a novel approach that grounds language models within structured representations derived from open-vocabulary scene graphs, dynamically updated as the environment is explored. We tightly interleave these representations with an object-centric action space. The resulting approach is zero-shot, open-vocabulary, and readily extendable to a spectrum of mobile manipulation and household robotic tasks. We demonstrate the effectiveness of MoMa-LLM in a novel semantic interactive search task in large realistic indoor environments. In extensive experiments in both simulation and the real world, we show substantially improved search efficiency compared to conventional baselines and state-of-the-art approaches, as well as its applicability to more abstract tasks. We make the code publicly available at <http://moma-llm.cs.uni-freiburg.de>.

## I. INTRODUCTION

Interactive embodied AI tasks in large, unexplored, human-centered environments require reasoning over long horizons and a multitude of objects. In many cases, the considered environments are *a priori* unknown or continuously rearranged. Recent advancements have demonstrated the potential of large language models (LLMs) in generating high-level plans [1]–[4]. However, these efforts have predominantly focused on fully observed environments such as table-top manipulation, or *a priori* explored scenes, struggling to generate executable and grounded plans suitable for real-world robotic execution. This problem is strongly exacerbated in large scenes with numerous objects and long time horizons. In turn, this increases the risk of generating impractical sequences or hallucinations [5], [6]. Furthermore, the presence of interactive scenes and articulated objects introduces a multitude of potential states and failure cases. To address these challenges, we propose grounding LLMs in dynamically built scene graphs. Our approach incorporates a scene understanding module that constructs open-vocabulary scene graphs from dense maps and Voronoi graphs. These diverse representations are then tightly interwoven with an object-centric action space. Leveraging the current scene representation, we extract structured and compact textual representations of the scene to facilitate efficient planning with pre-trained LLMs.

To evaluate the efficacy of our approach, we formulate an interactive semantic search task, extending previous non-semantic interactive tasks [7] to more complex scenarios.

\* Equal contribution.

<sup>1</sup> Department of Computer Science, University of Freiburg, Germany.

<sup>2</sup> Toyota Motor Europe (TME).

This work was funded by Toyota Motor Europe (TME) and an academic grant from NVIDIA.

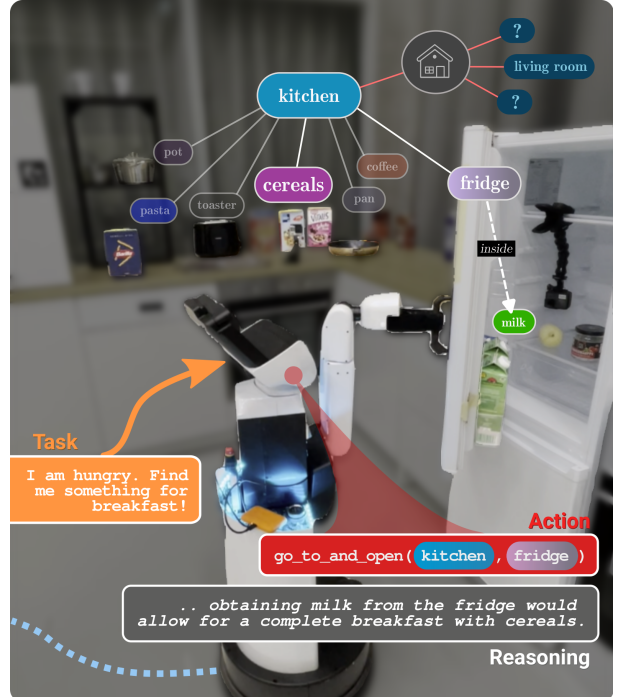


Fig. 1. MoMa-LLM performs long-horizon interactive object search in household environments from language queries using dynamically built scene graphs.

In this task, an agent has to find a target object within an indoor environment, encapsulating real-world challenges such as opening doors to navigate through the environment, and searching inside cabinets and drawers to find the desired object. This task is challenging as it requires reasoning about manipulation and navigation skills, operating in unexplored environments, spanning large apartments with numerous rooms and objects. Consequently, it is representative of more complex mobile manipulation tasks while retaining the specificity required for thorough evaluations and comparisons against conventional methods. Furthermore, we introduce a novel evaluation paradigm for object search tasks, employing full efficiency curves to remove the dependency on arbitrary time budgets inherent in existing methods. Additionally, we propose the *AUC-E* metric to distill these curves into a single metric for coherent evaluation. We perform extensive experimental evaluations in both simulation and the real-world, and demonstrate that given appropriately structured representations, LLMs can leverage their accumulated knowledge about the human world to achieve exceptional results, outperforming state-of-the-art approaches across diverse fields. Our approach is zero-shot, open-vocabulary, and inherently scalable to various mobile manipulation and household robotic tasks, as we demonstrate on a set of abstract search tasks.

To summarize, our main contributions are

- A scalable scene representation centered around a dynamic

scene graph with open-vocabulary room clustering and classification.

- Structured compact knowledge extraction to ground LLMs in scene graphs for large unexplored environments.
- Semantic interactive search task for large scenes with numerous objects and receptacles.
- Novel evaluation paradigm for object search tasks through full efficiency curves, instead of a single time budget.
- We make the code publicly available at <http://moma-llm.cs.uni-freiburg.de>.

## II. RELATED WORK

*3D Scene Graphs* serve as sparse environment representations that abstract from dense semantic [8] or panoptic maps [9]. The disassembly of large scenes into objects, regions, etc., and their representation as nodes thus provides hierarchical and object-centric representations. In addition, nodes and edges may contain semantic attributes [10]–[13]. Despite the lower geometric fidelity compared to dense maps, scene graphs prove particularly successful in the realm of high-level reasoning and planning, while providing a powerful interface with mapping [5], [12]. Orthogonally, Hydra [10] focuses on representing dynamically changing scenes. Multiple works have explored the use of scene graphs for reasoning in mobile robotics. Most build a hierarchical scene graph of the form (building, floors, rooms, objects). Different variants add edges among objects [14], add a Voronoi graph [15] for storing observations, or separate the set of objects into static and potentially moving objects [16]. While ConceptGraphs [14] and VoroNav [15] investigate the use of zero-shot perception inputs for task planning, others such as SayPlan [5], SayNav [16], and Taskography [6] focus on the reasoning task itself by utilizing ground truth semantic scene graphs [17], [18]. Realizing object navigation using both dynamic and interactive scene graphs has not been tackled thus far in the aforementioned works.

*Language Models for Planning*: Several recent works have investigated language models' abilities to generate task plans for robotic manipulation. These largely focus either on static table-top scenes of limited size and a limited number of objects [1], [3], [4], or a fully observable scene. On the other side of the spectrum, vision-language-navigation investigates pure navigation tasks in large apartments to either navigate along a described path or towards a specific instance of an object [19], [20]. A smaller number of works have investigated apartment-wide mobile manipulation tasks. LLM-Planner [20] uses information retrieval of the closest matching known task. Chalvatzaki *et al.* [18] finetune an LLM to encode object-object relations extracted from a scene graph. SayCan [21] combines affordance values with language scores. However, all of these methods focus on tasks restricted to single rooms. SayPlan [5] focuses on identifying relevant subgraphs in large known scene graphs by iteratively extracting or collapsing nodes. Ni *et al.* [17] learn a transformer-based model on top of a frozen LLM to predict subtasks from fully known scene graphs. In contrast, we focus on interactive search in large fully unexplored environments. As a result, simple prompting strategies, such as providing a list of observed objects [14], [17], [20] or raw JSON input [5] of a full scene graph to a

language model becomes insufficient, as we demonstrate in our experiments.

*Object Search* has been tackled via a wide range of methods, including classical methods such as frontier exploration [22], vision-based reinforcement learning [23], or auditory signals [24]. Graph Neural networks (GNNs) have been used with scene graphs to find specific object instances with hierarchical and relational constraints [25] or in frequently changing, dynamic scenes [26], [27]. Schmalstieg *et al.* [7] introduced the interactive search task, in which an agent has to open doors and search through cabinets and drawers. While they focus on random target placements and a restricted number of objects and receptacles, we introduce a semantic single-object search variation of this task, which uses all objects in the scene and keeps the semantic co-occurrences in the scene intact.

Non-interactive semantic search has been previously tackled. Most recent methods used language models to extract similarities or co-occurrences with the target object to score frontiers [28]–[30] or predict potential functions towards a target object with supervised learning [31]. While these works focus on pairwise score calculations, we treat it as a planning problem in which the full scene is encoded jointly. In contrast to these works, we consider objects that are not freely accessible and require interaction with the environment and thereby reasoning over multiple steps such as opening doors and receptacles instead of pure directional reasoning. Lastly, our approach is fully open-vocabulary - both in terms of room and object categories. Conceptually most similar to our work, SayNav [16] utilizes a scene graph together with an LLM. However, it focuses on non-interactive search, restricting the LLM's access to a room subgraph, assumes restrictions such as knowledge about scene graph edges, and relies on a hardcoded heuristic of when to go to the next (already open) door.

## III. PROBLEM STATEMENT: EMBODIED REASONING

In our setting, an embodied, robotic agent is situated in a large, unexplored environment and has to complete a given task, described by a language goal  $g$ . The agent is acting in a Partially Observable Markov Decision Process (POMDP)  $\mathcal{M} = (\mathcal{S}, \mathcal{A}, \mathcal{O}, T(s'|s, a), P(o|s), r(s, a))$  where  $\mathcal{S}, \mathcal{A}$  and  $\mathcal{O}$  are the state, action and observation spaces,  $T$  and  $P$  describe the transition and observation probabilities,  $s, s'$  are the current and next state,  $o$  is the current observation,  $a$  is the current action and  $r$  is the reward. To succeed in these tasks, the agent has to perceive the environment and create a representation while reasoning about how to complete the tasks through exploration and interaction with the environment.

We introduce the task of *semantic interactive object search*. In contrast to most existing works [23], [28], [29], [32], interactive object search requires manipulation of the environment to navigate and explore it. As in realistic, human-centric environments, doors may block pathways and objects are not openly visible but may be stored away in receptacles like drawers or cabinets. We extend the interactive task introduced in [7] to a much larger number of objects and receptacles and a prior distribution of realistic room-object and object-object relations. As a result, other objects in the scene can provide valuable information about the position of the target. While

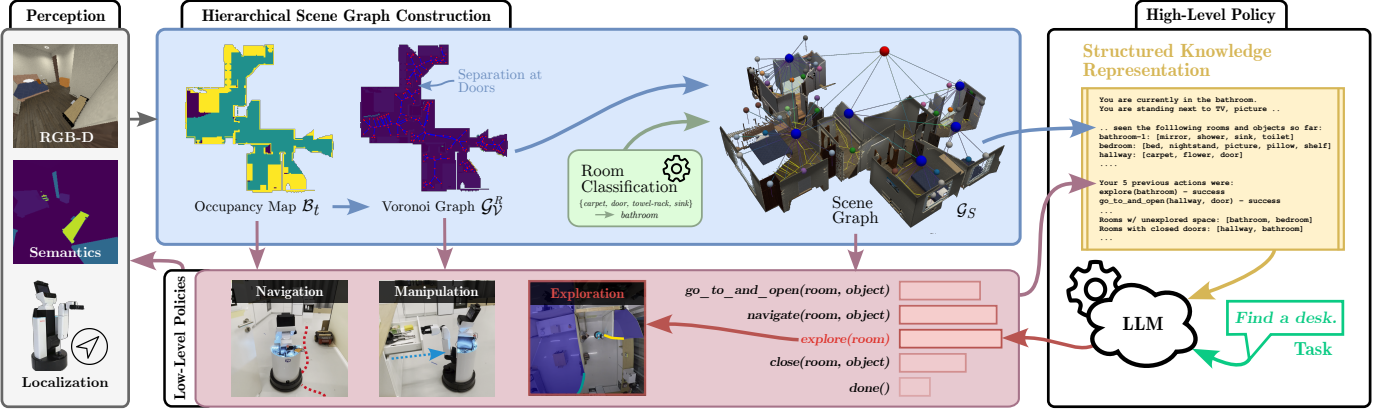


Fig. 2. MoMa-LLM: From posed RGB-D images and semantics, we construct a semantic 3D map from which we extract a various occupancy maps in the BEV space and construct a navigational Voronoi graph. Through room clustering and room-object assignments we then build up a hierarchical scene graph. From this scalable scene representation, we extract the task-relevant knowledge and encode it into a structured language representation. A large language model then produces high-level commands which are executed by low-level subpolicies. These in turn draw on and update the scene representations.

existing tasks such as the Habitat challenge and Robothor use semantic placements, they do not support any physical interactions or objects placed within receptacles.

We implement the task in the iGibson scenes [33], consisting of 15 interactive apartments based on scans of real houses. At the beginning of an episode, all doors are closed and the agent is given a task description in natural language. The task is deemed successful if the agent has observed an instance of the target category and calls `done()`. The iGibson scenes contain realistic furniture and room distributions, but few other objects are placed in relation to this. We provide a method to enrich the scenes with realistic object placements, both within receptacles and on top of furniture, by extending and matching previously introduced prior distributions  $P^{prior}$  over room and object relations [26]. Given a valid scene instantiation, we then draw a target category  $g \sim U(\text{scene})$  from all categories in the scene. This results in the procedural generation of a wide range of tasks over 84 possible target classes. Full details can be found in the Supplementary Material Sec. S.1.

#### IV. MOMA-LLM

To address the challenges of interactive open-vocabulary household tasks, we propose *MoMa-LLM*, which intertwines high-level reasoning with scalable dynamic scene representations. We ground large-language models in hierarchical 3D scene graphs  $\mathcal{G}_S$  that hold object- and room-level entities as well as a more fine-grained Voronoi graph for navigation. The LLM provides high-level actions that are executed through low-level skills as shown in Fig. 2. In general, we assume access to ground truth perception as the focus of this work is on the reasoning aspect.

##### A. Hierarchical 3D Scene Graph

To provide an LLM with structured input, we craft a hierarchical scene graph that includes a navigational Voronoi graph.

1) *Dynamic RGB-D Mapping*: The agent perceives posed RGB-D frames  $\{I_0, \dots, I_t\}$  including semantics from the environment. The contained points are transformed into the global coordinate frame and arranged on a 3D voxel grid  $\mathcal{M}_t$ . As we tackle an interactive problem, our map is dynamically

updated based on novel explored areas or the occurrence of object dynamics in the scene. To infer obstacle positions, walls and explored free space, we first obtain the highest occupied entry per stixel in  $\mathcal{M}_t$ . These entries are then turned into a two-dimensional bird's-eye-view (BEV) occupancy map  $\mathcal{B}_t$  by inferring all occupied positions except for those classified as free space  $\mathcal{F}_t$ . The latter in turn represents the navigable area that is used for robot exploration.

2) *Voronoi Graph*: Subsequently, we abstract from the created dense maps by computing a navigational graph  $\mathcal{G}_V$  that is used in downstream tasks to associate objects in close vicinity or estimate geodesic distances. We first inflate  $\mathcal{B}_t$  using an Euclidean signed distance field (ESDF) formulation for robustness, but overwrite free space coordinates as given in  $\mathcal{F}_t$  as zero. Based on this, we compute a Generalized Voronoi Diagram (GVD) that holds a set of points  $\mathcal{V}$  with the same clearance to the closest obstacles:

$$\mathcal{V} = \{p \in \mathcal{F}_t \mid \{q \in \mathcal{B}_t \mid d(q, p) = \min_{q \in \mathcal{B}_t} d(q, p)\}\}, \quad (1)$$

where obstacle points  $q$  are drawn from  $\mathcal{B}_t$ . After obtaining  $\mathcal{V}$ , we exclude all nodes that lie in the immediate vicinity of obstacles or do not reside within the occupied map boundaries. Given the path of obtained medial axes, we then construct edges  $\mathcal{E}$  among  $\mathcal{V}$  and obtain our navigational Voronoi graph  $\mathcal{G}_V = (\mathcal{V}, \mathcal{E})$ . Throughout our experiments, we found that extracting the largest connected component of the graph provides the robot-centric Voronoi graph while other components commonly lie outside the explored area. Lastly, we sparsify  $\mathcal{G}_V$  to obtain fewer navigational nodes.

3) *3D Scene Graph*: The MoMa-LLM-policy operates on an attributed 3D scene graph  $\mathcal{G}_S$  that holds different abstraction levels, namely rooms and objects. We first separate the global Voronoi graph  $\mathcal{G}_V$  into multiple regions. To do so, we eliminate edges and nodes of  $\mathcal{G}_V$  near doors. Using a mixture of Gaussians, we generate a two-dimensional probability distribution over all observed doors in the environment:

$$\rho_{\mathcal{N}}(\mathbf{x}, \mathbf{H}) = \frac{1}{N_D} \sum_{i=1}^{N_D} K_{\mathbf{H}}(\mathbf{x} - \mathbf{x}_i), \quad (2)$$

where  $\mathbf{x}_i = (x_i, y_i)$  are the door center coordinates,  $K_{\mathbf{H}}$  is the scaled Gaussian kernel of observed doors and  $\mathbf{H}$  the

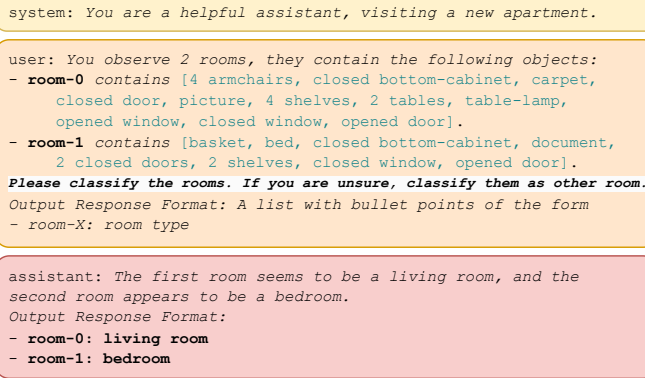


Fig. 3. Room Classification Prompt: based on the objects and room clusters of the scene graph, an LLM performs open-vocabulary classification.

bandwidth matrix. Edges that exceed an empirically tuned probability threshold are disregarded along with isolated nodes. Following this principle, we obtain the separated Voronoi graph  $\mathcal{G}_V^R$  covering distinct rooms. In the next step, we infer the high-level connectivity among rooms by calculating the shortest paths between nodes of  $\mathcal{G}_V$  that belong to disjoint components of  $\mathcal{G}_V^R$ . Whenever a path *traverses* just two distinct rooms as given by  $\mathcal{G}_V^R$ , the two rooms count as immediate neighbors. Finally, we map objects to rooms. For each object  $o \in \mathcal{G}_S$ , we identify the node  $n_R \in \mathcal{G}_V^R$  that minimizes the distance to the closest viewpoint  $v_p$  from which the object was seen. To do so, we calculate the shortest path from the object  $o$  to this viewpoint, which consists of the path on the Voronoi graph and the Euclidean distance  $d$  from the Voronoi nodes to the object and viewpoint, respectively. By weighting the distance to the object with an exponent of  $\lambda = 1.3$ , we ensure to prefer nodes close to the object. Based on Eq. (3), objects are then assigned to the room label of the node  $n_R$  in  $\mathcal{G}_V^R$ . This prohibits the erroneous assignments of objects to a neighboring room through walls. Doors may be connected to multiple rooms.

$$n^R = \arg \min_{n_o \in \mathcal{G}_V^R} \text{path}(n_o, n_{v_p}) + d(o, n_o)^\lambda + d(v_p, n_{v_p}) \quad (3)$$

4) *Room Classification*: Similar to Chen *et al.* [34], we perform room classification by providing an LLM with the set of object categories contained in each room. We perform this as open-set classification, in which we let the LLM freely pick the room categories deemed most appropriate. The resulting LLM prompts are detailed in Fig. 3. Room classification is performed in each high-level policy step, as the explored scene and scene graph evolve.

### B. High-Level Action Space

We design an object-centric action space, which is tightly intertwined with the different granularities of the scene representation. It consists of the following high-level actions:

*navigate(room\_name, object\_name)*: Navigation to an object in a room via an A\* planner in the explored BEV-map  $\mathcal{B}_t$ , inflated by 0.1 m. It first navigates to the Voronoi node associated with the object, then to the most central, free point on an arc around the object. This enables robust navigation to objects in partially explored space and ensures navigation to the correct room through the Voronoi assignment detailed in

Sec. IV-A3. Navigation is considered successful if the agent reaches within 1.5 m of the object.

*go\_to\_and\_open(room\_name, object\_name)*: Navigate to a specific object, then open it. For doors, continue to navigate into the opened door frame.

*close(room\_name, object\_name)*: Equivalent to the opening action.

*explore(room\_name)*: Move to an unexplored frontier within this room. Deemed successful if the agent reaches within 0.5 m of the frontier point.

*done()*: Terminate the episode and evaluate if the target object has been found.

Ambiguities of multiple instances of the specified class in a room are resolved by selecting the closest instance. The subpolicies then generate actions in the low-level action space and return once they succeed or encounter a failure. Throughout their execution, they continuously update the scene representations. Refer to the Supplementary Material Sec. S.1 for details.

### C. Grounded High-Level Planning

We encode the accumulated knowledge of the scene graph into natural language by extracting the relevant components and embedding them in a problem-specific structured manner. Our method fulfills three properties: (i) grounding - guiding the LLM to adhere to the physical realities of the scene, (ii) specificity - avoiding long or irrelevant context queries that increase hallucinations and the difficulty of the planning problem [5], [6], and (iii) open-set - our method is open-vocabulary and performs in a zero-shot manner, enabling direct deployment with unknown semantics and perception models. The resulting prompt for the language model is shown in Fig. 4. In the following, we describe the main components of structured encoding. We demonstrate the importance of this structure in Sec. V.

1) *Scene Structure*: We encode the main room-object structure from the scene graph into a structured list of rooms and their containing objects and encode path distances (based on an A\*-planner) by binning them and mapping them to adjectives [18], as detailed in Supplementary Material Sec. S.3. We then employ the following filtering to allow for compact text encodings: we summarize matching nodes within a room with a counter, we filter out open doors that provide no new connectivity, and we encode object states directly within the object name, e.g. as "opened" or "closed [object-name]".

2) *Partial Observability*: As the environment is initially unknown, it requires explicit reasoning about exploration-exploitation trade-offs. We identify frontiers to explorable areas [22], then leverage the scene graph to provide them with semantic meaning. Firstly, we associate each frontier with a room through matching with  $\mathcal{G}_V^R$ . Secondly, we apply hole-filling to the BEV map to differentiate whether a frontier is an encapsulated area within a room, such as occluded space behind furniture, or whether the frontier is leading out to new areas. Correspondingly, we then represent them as "unexplored area" within a room, while frontiers that lead to other areas are listed separately, see Fig. 4. The second type of unexplored space is receptacles that may contain target objects. Together

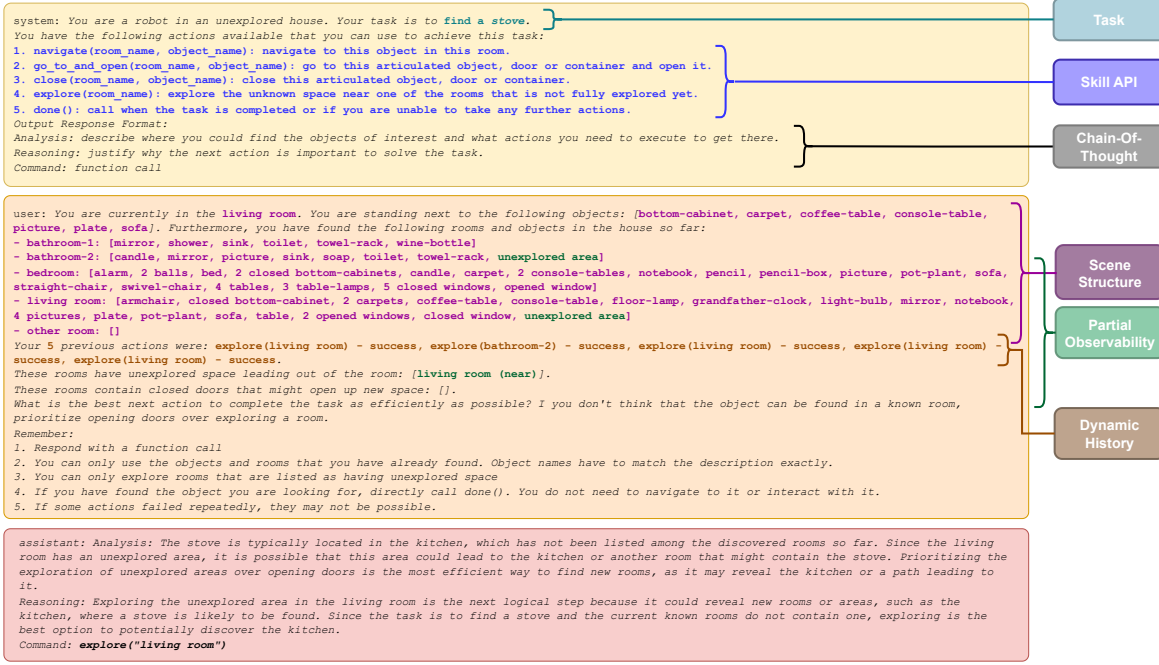


Fig. 4. High-level Reasoning Prompt: We encode the extracted scene representation to natural language, providing structured information to a language model.

with the encoded object states, we find that the language model is capable of inferring affordances from the object descriptions, removing the need to explicitly encode them. If trying to open objects that cannot be opened, the according subpolicy will fail and the LLM has to reason about an appropriate response.

3) *History in Dynamic Scenes*: Given the size of the scenes, the conversation history quickly grows too large to provide to a language model directly. Instead, we aim to find the most compact representation of previous actions to fulfill the Markov property. For each high-level decision, we encode the latest scene representation and start a new query to the LLM. As the scene representation is dynamically updated, this automatically encodes all newly acquired knowledge. To account for previous interactions, we provide the LLM with a history of the last  $h$  actions. But as the scene graph changes dynamically, the previous room- and object-centric function calls may no longer match the current scene. Instead, we keep track of interaction positions, and then re-align the previous actions by matching the positions to their closest Voronoi nodes and associated room labels. We then provide the LLM with a list of the re-aligned function calls, as shown in Fig. 4.

4) *Re-trial and Re-planning*: Extracting meaningful feedback for failure reasons for robots in the real world remains an open problem [2], as the number of possible failure reasons is almost unlimited. Instead, we provide very limited feedback about subpolicy success, which can be readily generated in the real world. We rely on a simple success state to the action history, stating “*success*”, “*failure*”, or “*invalid argument*” in case the output of the LLM could not be matched to the scene graph. We differentiate two cases of replanning: if the agent attempted interactions or commands that cannot be parsed or are deemed infeasible without attempting execution, we have not gained any new information about the scene, and we continue the conversation with the message “*The last action*

*<function-call> failed. Please try another command.*”. In case of more than five failures without state change, we terminate the episode as unsuccessful. If a subpolicy attempted execution but failed to complete its task, we re-encode the latest scene, update the action history, and let the LLM make a normal next decision with the updated state.

## V. EXPERIMENTS

As language models, we use *gpt-4-1106-preview* for the high-level reasoning and *gpt-3.5-turbo-1106* for the simpler room classification task [35].

*Baselines*: We compare our approach against heuristic-based and recent learning-based and language-based methods. In contrast to our method, we provide all baselines except Unstructured LLM with a ground truth `done()` decision when the object has been observed.

*Random*: uniform random choice among all available actions.

*Greedy*: greedily triggers the closest feasible action.

*ESC-Interactable*: ESC is a recent approach for semantic object search [28] which scores frontiers based on object-object and object-room co-occurrences as well as their distance. We extend the approach to interactive search by using the same rules to score openable objects and then select the action with the highest value. Co-occurrences are based on similarities of a finetuned Deberta-v3 language model [36], following the authors’ instructions. To isolate the impact of the decision making, we use the same scene graph and low-level policies as for our method.

*HIMOS*: A hierarchical reinforcement learning approach [7] which learns to combine frozen low-level policies for interactive object search, based on a semantic map memory. We adapt it by giving it the same subpolicies as our approach and scale it to the much larger number of objects in our scenes by restricting the instance navigation to target and articulated objects.

TABLE I  
INTERACTIVE OBJECT SEARCH RESULTS IN SIMULATION

Model	SR	SPL	AUC-E	Object Interactions	Distance Traveled	Infeasible Actions
Random	88.8	45.8	71.8	7.0	42.4	–
Greedy	81.1	47.2	68.8	8.6	24.7	–
ESC-Interactive	90.3	52.0	<u>77.5</u>	5.8	28.2	–
HIMOS	<b>93.1</b>	47.5	<u>75.7</u>	5.3	43.2	–
Unstructured LLM	81.4	<u>55.0</u>	72.8	<b>3.9</b>	<b>19.2</b>	<u>0.51</u>
MoMa-LLM (ours)	<u>92.6</u>	<b>59.9</b>	<b>82.5</b>	<u>4.2</u>	<b>19.2</b>	<u>0.35</u>

Notes: Best and second best highlighted in bold and underline. Object interactions, distance travelled and infeasible actions averaged over all episodes - including early terminated failures. Infeasible Actions: average number of steps the LLM produced an action that could not be executed, resulting in re-planning with continued conversation (cf. Sec. IV-C.4).

*Unstructured LLM*: This baseline provides the scene graph in a JSON format without any additional structure to the language model. The prompt structure is derived from SayPlan [5], adapted to the instructions and scene graph of our method. See Supplementary Material Sec. S.4 for a prompt example.

*Metrics*: We use three types of metrics to evaluate methods. *Success rate (SR)*: the share of episodes in which the agent finds the target object. We terminate an episode if the agent reaches 50 high-level steps, indicating being stuck.

*Success weighted by Path Length (SPL)*: A common metric for evaluation of search efficiency [37]. The metric calculates the fraction of distance traveled to the shortest possible path and weights it by whether the episode was successful. This metric does not take into account the costs of object interactions.

*Search efficiency curve and AUC-E*: While the commonly used success and SPL metrics allow for reducing the evaluation to a single number, they rely on an arbitrarily set maximum allowed time budget or number of environment steps.

As a result, these metrics do not differentiate between methods that search thoroughly but on average take more steps versus methods that search large areas very quickly, but that might fail to search every corner for small objects. Instead, we reason that the desired time budget depends heavily on the use case and propose a new metric that evaluates the full efficiency curve. For each possible budget (number of steps), we calculate the share of episodes that succeeded with this or fewer number of steps. This results in an efficiency curve, in which the best policies are located in the top left corner, enabling the comparison of success rates for arbitrary budgets. We can still reduce this to a single number by calculating the area under the efficiency curve (AUC-E). A perfect (but unachievable) policy, that finds all objects in a single step will have a value of one, a policy that does not find any objects will have a value of zero. We calculate the integral up to 5,000 low-level steps, at which points almost all methods make no further progress.

### A. Simulation Experiments

We instantiate the task in the iGibson simulator [33] with a Fetch robot. In contrast to previous LLM-based works [5], [16], we evaluate all approaches in completely unseen apartments, following the data split of the iGibson challenge into eight training scenes for the development of all modules and

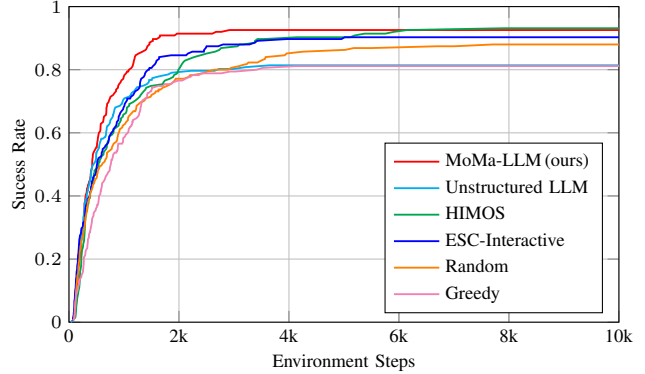


Fig. 5. Interactive search efficiency curve in simulation. Each point depicts the success rate for a given maximum time budget (x-axis).

prompt engineering and seven test scenes. For each scene, we evaluate the agent over 25 procedurally generated episodes with randomized start poses, target objects, and object distributions.

*Scene Understanding*: We measure the graph purity of obtained per-room Voronoi graph nodes with respect to the ground truth floor plans to measure the scene graph accuracy. As the scene graph is constructed dynamically, we evaluate each high-level policy step and obtain an average purity of 0.609 across all test scenes. We found our policy to be robust to under-segmented rooms even though objects from multiple rooms were, e.g., considered part of a single room. By relying on the camera pose from which an object is observed we reduce the number of wrong object-room assignments *through* walls to a minimum. Following the door-wise separation of rooms, our approach however is prone to *open* room concepts such as combined kitchen and living rooms. For more information and graph depictions, refer to the Supplementary Material Sec. S.1.

*Policies*: The results and efficiency curves for the search task are shown in Tab. I and Fig. 5. We find that, given appropriate subpolicies, heuristics can complete a significant share of episodes. However, they are not sufficient for an efficient search strategy, resulting in low SPL and AUC-E. Similarly, while HIMOS achieves a higher success rate, it is unable to explore efficiently. We found that the RL agent struggled with the much larger action space that resulted from the many more interactable instances in our scenes than in the original work. ESC in contrast, is able to exploit the co-occurrences to improve over the other baselines. However, given its pairwise comparisons, is unable to optimize over longer action sequences. In contrast, MoMa-LLM achieves similar success rates as HIMOS with a much higher search efficiency, both in terms of SPL and AUC-E. We find that the structured prompt representation is essential for this, with the Unstructured LLM performing much worse.

This picture is fortified by the full efficiency curves in Fig. 5, which show that MoMa-LLM achieves the highest performance for all given time budgets. In contrast, random heuristics achieve very high coverage, resulting in good success rates, but often take very long to find specific objects. Further examining the different models, we find that MoMa-LLM both travel much shorter distances and open fewer objects on average, indicating efficient and target-driven behavior. In

TABLE II  
RESULTS ON THE FUZZY SEARCH TASKS IN THE REAL WORLD.

Task	Success	Reasoning
I am hungry. Find me something for breakfast.	✓	Found cereals, toast, coffee. Then opened fridge to look for milk or eggs. Found milk in the fridge and decided these are sufficient items.
Find me something to wash my hands.	✓	Searched kitchen for a sink. When not finding one, searches for storage room or bathroom until it finds the sink in the bathroom.
I feel sleepy. Find me something to wake up. Find things to set the kitchen table.	✓ ✓	The teapot is associated with tea that contains caffeine and can help someone wake up. Explored kitchen, opening cabinets. Found knife, glasses, plates. Continued to look for forks or spoons. When not finding them, called done. (No forks or spoons existed).
Find me the book in the living room.	✓	Explored until finding living room, then opened cabinet looking for book, found it inside.
Pour me a glass of milk.	✓	Finds milk in fridge, glass on table. Navigates between the two, assuming to transport the last object. Then terminates, reasoning that it has found and navigated to both.
Turn on the oven. What's the time?	✓ ✓	Finds the oven and calls done(): "Turning on oven is implied as completion of the task". Finds the clock and calls done(): "The clock is the object that will provide the time".

Notes: Top: fuzzy search queries. Bottom: infeasible task queries. Success in these tasks is evaluated by human judgment as a reasonable response. The reasoning has been qualitatively paraphrased for brevity.

contrast, Unstructured LLM produces almost 50% more invalid actions. Qualitatively, we find that MoMa-LLM is robust to various room layouts, such as "combined kitchen and living rooms" that result in very large room clusterings and can handle the open-vocabulary room classification well. For reasoning examples, refer to the Supplementary Material Sec. S.5.

### B. Real-World Experiments

We then transfer our policy to the real world. We create a real-world apartment, consisting of four rooms: a combined kitchen and dining room, a living room, a long hallway, and a bathroom. We use a Toyota HSR robot, equipped with an RGB-D camera and a 270° LiDAR. We replace the navigation policies with the ROS Nav Stack and the manipulation actions with the N<sup>2</sup>M<sup>2</sup> manipulation policies [38]. We rely on the same assumptions as in simulation and assume access to localization, accurate semantic perception, and handle detection. We implement this by pre-recording a map with the robot's LiDAR and annotating it with semantic labels. At test time, we create an occupancy map from the robot's RGBD camera and reveal the corresponding part of the semantic map to the agent. The pre-recorded map is also used for localization. To detect handles, we use AR-Markers placed on each object. For details refer to the Supplementary Material Sec. S.2.

We evaluate both MoMa-LLM and the most efficient baseline, ESC. The results are shown in Tab. III, Fig. 6, and the accompanying video. Both methods succeeded in 8/10 episodes, demonstrating the successful transfer of the system to the real world. We find that the Voronoi- and scene graph construction transfer directly to the unseen and quite different layout. Similarly, the system directly transfers to the change in subpolicies, where the mobile manipulation policies ensure a successful transition between all subpolicies. The two failures stemmed from irrecoverable failures of the subpolicies, in particular, collisions of the base during navigation or of the arm while opening the door. Comparing the two methods, we find confirmation of the simulation results, with MoMa-LLM moving and opening objects more target-driven and efficient. Furthermore, the agent was able to react to the (unseen) failure cases of the subpolicies, such as re-trying to open a drawer when the gripper slipped off the handle.

TABLE III  
INTERACTIVE OBJECT SEARCH RESULTS IN THE REAL WORLD

Model	Success Rate	Navig Fails	Manip Fails	Distance Traveled	Object Interact.
ESC-Inter.	80%	2	0	33.9	3.5
MoMa-LLM	80%	1	1	<b>17.9</b>	<b>2.2</b>

Notes: Dist. travelled is the average distance travelled per episode in meters. Object interactions are the average number of object interactions per episode.



Fig. 6. We construct a real-world apartment covering four rooms and 54 objects and transfer the model to a Toyota HSR robot.

### C. Towards General Household Tasks

While heuristics can achieve reasonable results if endowed with an appropriate problem structure, as we move to more abstract and complex tasks, it becomes increasingly difficult to define problem-specific rules. In contrast, our approach is readily expandable to a wide range of household and mobile manipulation tasks. Representative of this, we introduce a *fuzzy search task*. In this task, the robot does not receive a specific object class to find, but rather a fuzzy description, such as an affordance. The queries are shown in Tab. II.

We find that the agent is capable of finding objects that satisfy respective queries, and correctly reasoning about task completion by calling *done()*. We further test this capability with three tasks that cannot be solved with the given subpolicies

(bottom part of Tab. II). For these cases, the agent terminated the episode after finding the relevant objects, reasoning that these objects would now be sufficient for further completion of the tasks. This demonstrates the flexibility of our approach. We leave the extension to arbitrary tasks to future work.

## VI. CONCLUSION

We developed a method to ground language models for high-level reasoning with scalable, dynamic scene graphs and efficient low-level policies for interactive tasks that require combined reasoning about manipulation, navigation and exploration. We demonstrated the importance of extracting structured knowledge for large and unexplored scenes and that given such a structured scene representation, LLMs can reason about efficient search strategies, outperforming fully learned or co-occurrence-based methods. We then transferred of our method to a real-world apartment, achieving consistent performance over many episodes. Lastly, we demonstrate the applicability and extendability of our approach to abstract tasks, opening the door towards general household tasks. Furthermore, we made the code publicly available to facilitate future research.

## ACKNOWLEDGEMENTS

We thank Aron Distelzweig for his help in implementing the HIMOS model for this task.

## REFERENCES

- [1] W. Huang, C. Wang, R. Zhang, Y. Li, J. Wu, and L. Fei-Fei, “Voxposer: Composable 3d value maps for robotic manipulation with language models,” in *Proc. of the Conf. on Rob. Learning*, 2023.
- [2] Z. Liu, A. Bahety, and S. Song, “REFLECT: Summarizing robot experiences for failure explanation and correction,” in *Proc. of the Conf. on Rob. Learning*, 2023.
- [3] B. Li, P. Wu, P. Abbeel, and J. Malik, “Interactive task planning with language models,” in *2nd Workshop on Lang. and Robot Learning: Language as Grounding (CoRL)*, 2023.
- [4] K. Lin, C. Agia, T. Migimatsu, M. Pavone, and J. Bohg, “Text2motion: from natural language instructions to feasible plans,” *Autonomous Robots*, vol. 47, no. 8, pp. 1345–1365, 2023.
- [5] K. Rana, J. Haviland, S. Garg, J. Abou-Chakra *et al.*, “Sayplan: Grounding large language models using 3d scene graphs for scalable task planning,” *Proc. of the Conf. on Rob. Learning*, 2023.
- [6] C. Agia, K. Jatavallabhula, M. Khodeir, O. Miksik, V. Vineet *et al.*, “Taskography: Evaluating robot task planning over large 3d scene graphs,” in *Proc. of the Conf. on Rob. Learning*, 2022, pp. 46–58.
- [7] F. Schmalstieg, D. Honerkamp, T. Welschehold, and A. Valada, “Learning hierarchical interactive multi-object search for mobile manipulation,” *IEEE Robotics and Automation Letters*, 2023.
- [8] N. Gosala, K. Petek, P. L. Drews-Jr, W. Burgard, and A. Valada, “Skyeye: Self-supervised bird’s-eye-view semantic mapping using monocular frontal view images,” in *Proc. of the IEEE Conf. on Comp. Vision and Pattern Recognition*, 2023, pp. 14901–14910.
- [9] N. Vödisch, K. Petek, W. Burgard, and A. Valada, “Codeps: Online continual learning for depth estimation and panoptic segmentation,” in *Robotics: Science and Systems*, 2023.
- [10] N. Hughes, Y. Chang, and L. Carlone, “Hydra: A real-time spatial perception system for 3D scene graph construction and optimization,” in *Robotics: Science and Systems*, 2022.
- [11] I. Armeni, Z.-Y. He, A. Zamir, J. Gwak, J. Malik, M. Fischer, and S. Savarese, “3D scene graph: A structure for unified semantics, 3D space, and camera,” in *Int. Conf. on Computer Vision*, 2019.
- [12] E. Greve, M. Büchner, N. Vödisch, W. Burgard, and A. Valada, “Collaborative dynamic 3d scene graphs for automated driving,” *Int. Conf. on Robotics & Automation*, 2024.
- [13] S.-C. Wu, J. Wald, K. Tateno, N. Navab, and F. Tombari, “SceneGraph-Fusion: Incremental 3D scene graph prediction from RGB-D sequences,” in *Proc. of the IEEE Conf. on Comp. Vision and Pattern Recognition*, 2021, pp. 7515–7525.
- [14] Q. Gu, A. Kuwajerwala, S. Morin, K. M. Jatavallabhula, B. Sen *et al.*, “Conceptgraphs: Open-vocabulary 3d scene graphs for perception and planning,” *Int. Conf. on Robotics & Automation*, 2024.
- [15] P. Wu, Y. Mu, B. Wu, Y. Hou, J. Ma, S. Zhang, and C. Liu, “Voronav: Voronoi-based zero-shot object navigation with large language model,” *arXiv preprint arXiv:2401.02695*, 2024.
- [16] A. Rajavanshi, K. Sikka, X. Lin *et al.*, “Saynav: Grounding large language models for dynamic planning to navigation in new environments,” *arXiv preprint arXiv:2309.04077*, 2023.
- [17] Z. Ni, X.-X. Deng, C. Tai, X.-Y. Zhu, X. Wu, Y.-J. Liu, and L. Zeng, “Grid: Scene-graph-based instruction-driven robotic task planning,” *arXiv preprint arXiv:2309.07726*, 2023.
- [18] G. Chalvatzaki, A. Younes, D. Nandha, A. T. Le, L. F. Ribeiro, and I. Gurevych, “Learning to reason over scene graphs: a case study of finetuning gpt-2 into a robot language model for grounded task planning,” *Frontiers in Robotics and AI*, vol. 10, 2023.
- [19] J. Gu, E. Stefan, Q. Wu, J. Thomason, and X. Wang, “Vision-and-language navigation: A survey of tasks, methods, and future directions,” in *Proc. of the Assoc. for Computational Linguistics*, 2022, pp. 7606–7623.
- [20] C. H. Song, J. Wu, C. Washington, B. M. Sadler, W.-L. Chao, and Y. Su, “Llm-planner: Few-shot grounded planning for embodied agents with large language models,” in *Int. Conf. on Computer Vision*, 2023, pp. 2998–3009.
- [21] B. Ichter, A. Brohan, Y. Chebotar, C. Finn, K. Hausman *et al.*, “Do as i can, not as i say: Grounding language in robotic affordances,” in *Proc. of the Conf. on Rob. Learning*, 2022.
- [22] B. Yamauchi, “A frontier-based approach for autonomous exploration,” in *Proc. of the IEEE Int. Symp. on Comput. Intell. in Rob. and Aut.*, 1997.
- [23] D. S. Chaplot, D. Gandhi, S. Gupta, A. Gupta, and R. Salakhutdinov, “Learning to explore using active neural slam,” in *Int. Conf. on Learning Repr.*, 2020.
- [24] A. Younes, D. Honerkamp, T. Welschehold, and A. Valada, “Catch me if you hear me: Audio-visual navigation in complex unmapped environments with moving sounds,” *IEEE Robotics and Automation Letters*, vol. 8, no. 2, pp. 928–935, 2023.
- [25] M. Lingelbach, C. Li, M. Hwang, A. Kurenkov, A. Lou, R. Martín-Martín, R. Zhang, L. Fei-Fei, and J. Wu, “Task-driven graph attention for hierarchical relational object navigation,” in *Int. Conf. on Robotics & Automation*. IEEE, 2023, pp. 886–893.
- [26] A. Kurenkov, M. Lingelbach, T. Agarwal, E. Jin, C. Li, R. Zhang *et al.*, “Modeling dynamic environments with scene graph memory,” in *Int. Conf. on Machine Learning*, 2023, pp. 17976–17993.
- [27] Z. Ying, X. Yuan, B. Yang, Y. Song, Q. Xu, F. Zhou, and W. Sheng, “Rp-sg: Relation prediction in 3d scene graphs for unobserved objects localization,” *IEEE Robotics and Automation Letters*, 2023.
- [28] K. Zhou, K. Zheng, C. Pryor, Y. Shen, H. Jin, L. Getoor, and X. E. Wang, “Esc: Exploration with soft commonsense constraints for zero-shot object navigation,” *Int. Conf. on Machine Learning*, 2023.
- [29] J. Chen, G. Li, S. Kumar, B. Ghanem, and F. Yu, “How to not train your dragon: Training-free embodied object goal navigation with semantic frontiers,” *Robotics: Science and Systems*, 2023.
- [30] N. Yokoyama, S. Ha, D. Batra, J. Wang, and B. Bucher, “Vlfm: Vision-language frontier maps for zero-shot semantic navigation,” *Int. Conf. on Robotics & Automation*, 2024.
- [31] S. K. Ramakrishnan, D. S. Chaplot, Z. Al-Halah, J. Malik, and K. Grauman, “Poni: Potential functions for objectgoal navigation with interaction-free learning,” in *Proc. of the IEEE Conf. on Comp. Vision and Pattern Recognition*, 2022, pp. 18890–18900.
- [32] F. Schmalstieg, D. Honerkamp, T. Welschehold, and A. Valada, “Learning long-horizon robot exploration strategies for multi-object search in continuous action spaces,” in *Robotics Research*, 2022, pp. 52–66.
- [33] C. Li, F. Xia, R. Martín-Martín *et al.*, “igibson 2.0: Object-centric simulation for robot learning of everyday household tasks,” in *Proc. of the Conf. on Rob. Learning*, vol. 164, 08–11 Nov 2022, pp. 455–465.
- [34] W. Chen, S. Hu, R. Talak, and L. Carlone, “Leveraging large language models for robot 3d scene understanding,” *arXiv preprint arXiv:2209.05629*, 2022.
- [35] OpenAI, “Gpt-4 technical report,” *arXiv*, pp. 2303–08 774, 2023.
- [36] P. He, J. Gao, and W. Chen, “Debertav3: Improving deberta using electra-style pre-training with gradient-disentangled embedding sharing,” in *Int. Conf. on Learning Repr.*, 2022.
- [37] P. Anderson, A. Chang, D. S. Chaplot, A. Dosovitskiy, S. Gupta, V. Koltun, J. Kosecka, J. Malik *et al.*, “On evaluation of embodied navigation agents,” *arXiv preprint arXiv:1807.06757*, 2018.
- [38] D. Honerkamp, T. Welschehold, and A. Valada, “N<sup>2</sup>m<sup>2</sup>: Learning navigation for arbitrary mobile manipulation motions in unseen and dynamic environments,” *IEEE Transactions on Robotics*, 2023.

# Language-Grounded Dynamic Scene Graphs for Interactive Object Search with Mobile Manipulation

## - Supplementary Material -

Daniel Honerkamp<sup>1\*</sup>, Martin Büchner<sup>1\*</sup>, Fabien Despinoy<sup>2</sup>, Tim Welschehold<sup>1</sup>, Abhinav Valada<sup>1</sup>

In this supplementary material, we provide additional details on the simulation and real-world environments, the subpolicies, and the baselines. Moreover, we provide additional results from the experiments. Further examples of real-world experiments are also demonstrated in the video material.

### S.1. SIMULATION ENVIRONMENT

#### A. Modifications

We make the following modifications to the iGibson scenes:

- We close all exterior doors and filter them out of the scene graph as they lead out to empty space.
- We scale the size of the Fetch robot by a factor of 0.85 as otherwise it is too large to navigate a significant number of areas.
- We remove six doors that block the robot’s pathway when opening (*door\_52* in *Pomaria\_0\_int*, *door\_75* in scene *Beechwood\_1\_int* and *door\_106* in *Ihlen\_1\_int*, *door\_90* in *Merom\_1\_int*, *door\_138* and *door\_139* in *Wainscott\_0\_int*).
- We rename four object categories, with misleading asset names, such as renaming *breakfast\_table* (which can be found e.g. in bedrooms) to *table*.

#### B. Task Generation

We first align the rooms and objects with the prior distribution. We manually match room labels and use cosine similarities of object name embeddings to match objects. We embed the object names from the scene and from the prior distribution with SBERT [1]. We then define a match as a cosine similarity  $\leq 0.7$  and being in the top 50 matched categories. As  $P^{prior}$  only contains two “inside” relationships, we enrich these relationships by assuming that all objects that can be found on top of an object and that fit in size, can also be found inside it and vice-versa. This results in an extended distribution  $P^{prior,ext}$ . We then procedurally enrich each episode by drawing additional objects from the set of admissible room-object-relations for all existing furniture in the iGibson scenes. We keep drawing until the physical placement of a relation succeeds or the distribution is exhausted. Given a valid scene instantiation, we draw a target category

$g \sim U(scene)$  from all categories in the scene. We reject targets as infeasible if no target instance is reachable from the agent’s random start position. We also reject all episodes in which the target object is immediately visible.

#### C. Perception

The robot in simulation is equipped with a differential drive and an RGB-D camera with a resolution of  $256 \times 256$  pixels and a vertical field of view of  $120^\circ$ . As the focus of this work is on decision making, we abstract from imperfect perception and assume access to ground truth instances and semantic segmentation from the simulator. For a realistic detection range, we restrict all sensors (depth, semantics) to a maximum range of 5 m and set a threshold of 50 segmented pixels before an object is considered detected - except for objects with a volume below  $0.01 \text{ m}^3$ . We furthermore assume accurate detection of whether an articulated object is open or closed and assume that objects within receptacles are detected after opening the object. We construct all maps at a resolution of 0.075 m and detect the *floor* and *carpet* categories as free space.

#### D. Execution

All methods start by fully turning around in-place to initialize the scene graph.

*Low-level action space:* The subpolicies act in a low-level action space consisting of the following actions:

- move forward by 7.5 cm
- turn-left by up to 35 rad
- turn-right by up to 35 rad
- open articulated object
- close articulated object
- done: end the episode and evaluate the success

*Navigation:* To reduce run-time, navigation actions are executed without physical simulation, but rather by directly setting the state of the robot. If no complete path in free space exists, the navigation policy will consider unexplored areas as traversable and replan with newly revealed free space. It will return ‘failed’ if it cannot find a path or reaches too many replanning attempts.

*Object interactions:* We follow previous work [2], [7] and execute articulated object manipulations as “magic actions”. These actions directly set the joint values of the object to their minimum or maximum. In the calculation of the efficiency curves and AUC-E, we weigh these actions by a time factor of

\*These authors contributed equally.

<sup>1</sup>Department of Computer Science, University of Freiburg, Germany.

<sup>2</sup>Toyota Motor Europe (TME)

Project page: <http://moma-llm.cs.uni-freiburg.de>

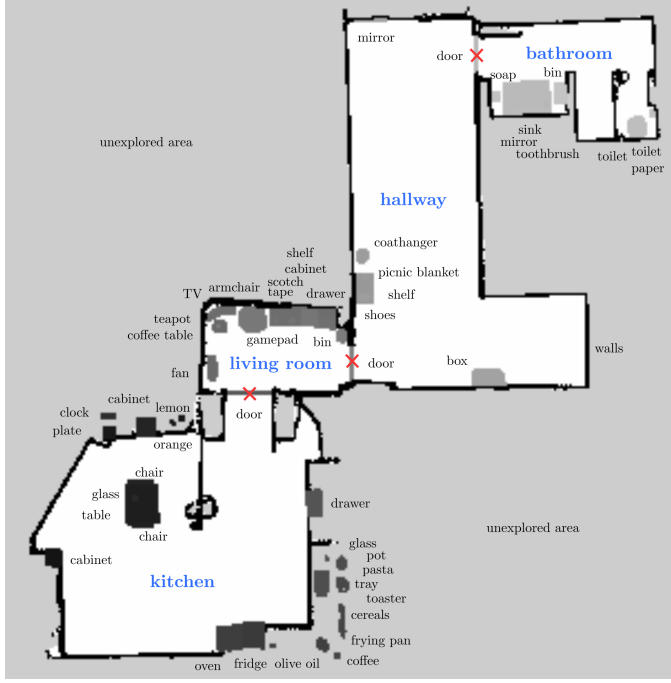


Fig. S.1. Map of the real-world environment. Different intensities represent different object instances in the environment. Room annotations are for illustration and not used by our model. Object labels denote approximate object positions.

30 to make their time cost comparable to an execution duration of roughly 30 seconds.

The `go_to_and_open()` action is implemented as follows:

- 1) Navigate to the Voronoi node closest to the object
- 2) Navigate to the most central free space in front of the object and turn toward it
- 3) Trigger the magic open action

## S.2. REAL-WORLD ENVIRONMENT

### A. Map

Fig. S.1 shows the map of the real-world environment. Different object instances are indicated in different intensities. The environment covers five different room types and 54 different object categories, including furniture such as tables, chairs, and a coat hanger, as well as small and less common objects such as soap, gamepad, or scotch tape. We set start positions for the robot in the kitchen, living room, and hallway. We ensure the same initial positions and targets for all methods.

### B. Execution

**Navigation:** We use the default manufacturer versions of the ROS NavStack as developed by Toyota for navigation. It uses the robot's LiDAR and depth cameras for dynamic obstacle detection and navigates in a map inflated by 0.25 m.

**Mobile manipulation:** Articulated object interactions are executed with pretrained  $N^2M^2$  manipulation policies [38]. The policy receives the handle pose, detected through AR-Markers,

TABLE S.1  
MAPPING OF DISTANCES TO NATURAL LANGUAGE.

$\leq$ Distance	Encoding
3.0	very close
10.0	near
20.0	far
$\infty$	distant

and uses a local occupancy map constructed from the LiDAR of the robot for obstacle avoidance. For each articulated object, we collect a single demonstration of opening the object. This demonstration consists of a set of poses of the robot's wrist link during the opening motion. These poses are then interpolated with splines to generate an end-effector motion. This agent's aim is to follow this end-effector motion to complete the object interaction. We evaluate whether the motion was successful based on whether the marker on the object changed its position after the execution of the subpolicy. For doors, we do not lock the spring-loaded door latch, as the robot is not strong enough to press the handle down.

The only exception to this is the door between the kitchen and living room. We found that the robot was unable to localize itself during the opening motion, as the moving door occupies the overwhelming majority of the robot's LiDAR measurements. As a result, it was not possible to follow the opening demonstration whenever the marker moved out of the robot's view. Instead, we use a simpler pushing motion from the inside and abstain from opening it in the other direction.

## S.3. LANGUAGE ENCODING

We encode distance to natural language based on a discrete mapping, following the principle of [18]. We bin the distance to the object, then apply the mapping reported in Tab. S.1. This results in a consistent relative language encoding.

## S.4. BASELINES

The *Unstructured LLM* baseline receives the same instructions and "remember" notes as our approach. The full JSON-formatted prompt of this baseline is depicted in Fig. S.2. We find that the much less structured and longer prompt leads to more frequent invalid actions or hallucinations (cf. Tab. I), such as trying to open objects that do not exist or are already opened. If stuck for repeated steps, this can result in failed episodes. A second source of failures are wrong terminations, in which the LLM calls `done()` while it has not found the correct object of interest.

## S.5. ADDITIONAL RESULTS

### A. Scene Graph Accuracy

Our proposed room separation scheme relies on separating Voronoi graphs at door positions. Thus, it is prone to under-segmentation whenever faced with open room layouts or, e.g.,

system: You are a robot in an unexplored house. Your task is to [find an oven](#). You have the following actions available that you can use to achieve this task:

1. `navigate(room_name, object_name):` navigate to this object in this room.
2. `go_to_and_open(room_name, object_name):` go to this articulated object, door or container and open it.
3. `close(room_name, object_name):` close this articulated object, door or container.
4. `explore(room_name):` explore the unknown space near one of the rooms that is not fully explored.
5. `done():` call when the task is completed or if you are unable to take any further actions.

**Output Response Format:**  
Analysis: describe where you could find the objects of interest and what actions you need to execute to get there.  
Reasoning: justify why the next action is important to solve the task.  
**Command:** function call

What is the best next action to complete the task as efficiently as possible? If you don't think that the object can be found in a known room, prioritize opening doors over exploring a room.

2. You can only use the objects and rooms that you have already found. Object names have to match the description exactly.
3. You can only explore rooms that are listed as having unexplored space
4. If you have found the object you are looking for, directly call done(). You do not need to navigate to it or interact with it.
5. If some actions failed repeatedly, they may not be possible.

assistant: Analysis:  
The oven is typically located in the kitchen, which is not explicitly listed in the scene graph. However, there are rooms that have not been explored yet, as indicated by the presence of frontier points. Since the oven has not been found in the known rooms and the priority is to open doors over exploring rooms when the object cannot be found in a known room, the next step should be to open any unopened doors that may lead to new rooms, potentially the kitchen.

The scene graph does not list any closed doors in the known rooms, but there are frontier points in the living room and bathroom-3 that suggest there are areas leading out or not fully explored. Since the living room has already been explored multiple times without finding an oven, and the bathroom is an unlikely location for an oven, the next logical step is to explore the frontier point in bathroom-3, which may lead to a new room.

Reasoning:  
Exploring the frontier point in bathroom-3 could reveal a new room, possibly the kitchen where the oven is likely to be found. Since the currently known rooms and there are no closed doors to open, exploring the frontier point is the next best action to potentially discover the kitchen.

Command:  
`explore(bathroom-3)`

TABLE S.2  
SCENE GRAPH EVALUATION

Environment	Open-Set	Purity $\mathcal{G}_V^R$	Room Category	Accuracy
iGibson	✗	0.609		0.276
Real-World	✓	-		0.901

*missing* doors to hallways. Downstream decision-making is performed at every high-level policy step, which requires accurate dynamically created scene graphs. Most importantly, the obtained representation varies a lot throughout the course of the exploration of the environment. In the following, all reported numbers denote the average across all high-level steps until an episode is finished to reflect this.

Tab. S.2 provides additional insights into the accuracy of the utilized scene graph representations. First, we evaluate

the purity of the separated Voronoi graph components by evaluating the underlying ground-truth room label per node in the simulation. The purity measures to which degree clusters only contain a single class. In our case, each separated Voronoi graph (representing a room) takes the role of a cluster. Next, we quantify how many ground-truth rooms are covered per the predicted Voronoi graph. Thus, the graph purity describes the degree of room under-segmentation apparent in the scene and thus measures how well door-wise Voronoi graph separation performs.

We observe an average purity throughout the exploration of 0.609 over 10 episodes across each of the iGibson test scenes. Nonetheless, open room layouts still pose a considerable hurdle, which would require additional perception inputs. More general approaches to segment rooms in the iGibson environments have shown inferior results. This is due to a large number of long and narrow corridors, which are hard to segment using classical

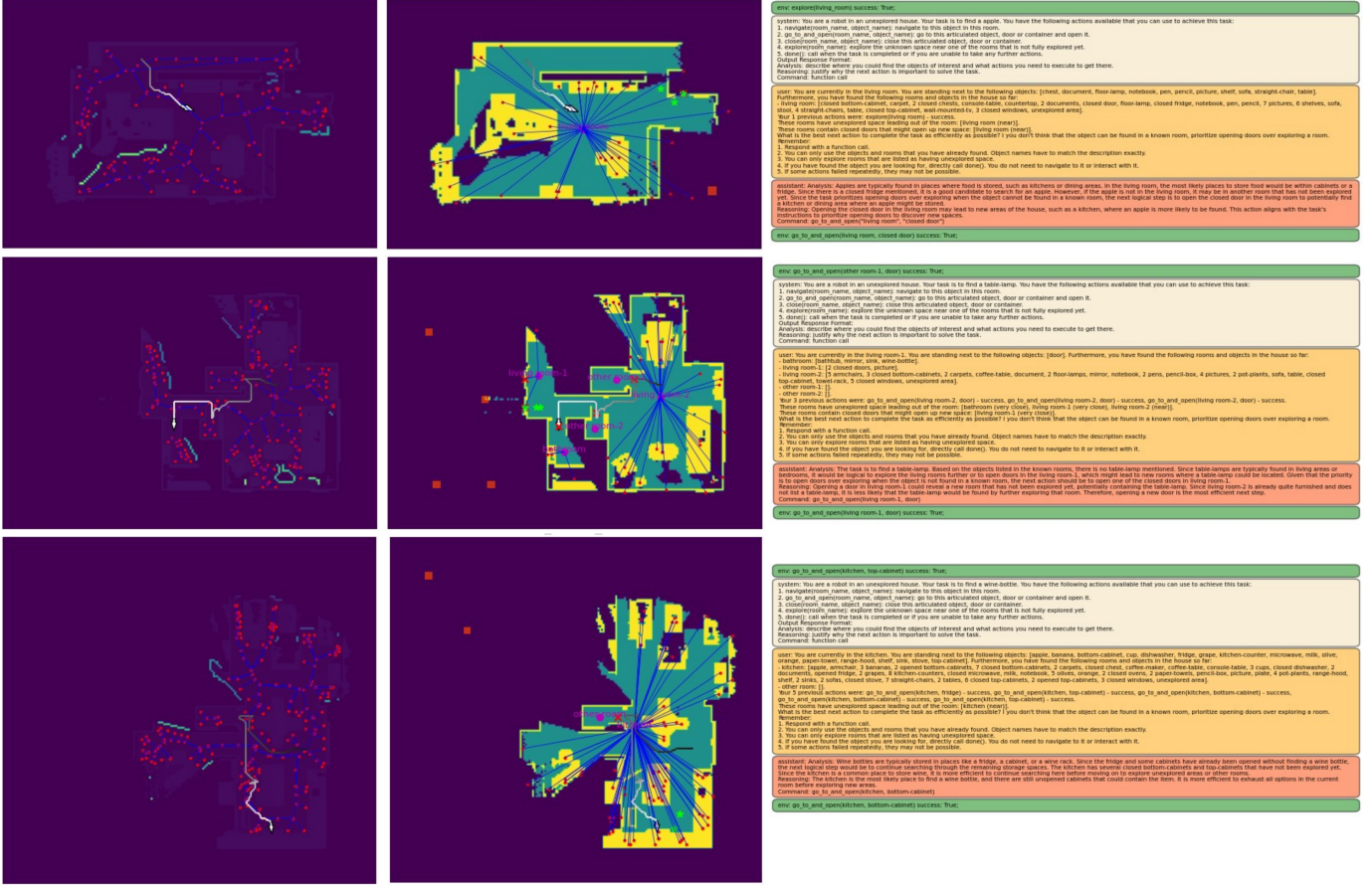


Fig. S.3. Examples of the reasoning of Voronoi graph and identified frontiers (left), scene graph (middle), MoMa-LLM (left). The green environment feedback is not provided to the LLM. Black-white: agent trace, red crosses: closed doors, red rectangles: undiscovered target objects, green stars: next selected navigation / interaction points. The bottom figure illustrates a suboptimal room clustering, which results in a very large room. We find the model to be robust against these clusterings.

morphological segmentation algorithms. Nonetheless, we found our policy to be robust to under-segmented rooms even though objects from multiple rooms were, e.g., considered part of a single room. By relying on the camera pose from which an object is observed we reduce the number of false object-room assignments (*through* walls) to a minimum. We show multiple resulting Voronoi graphs in Fig. S.3. In addition to the graph purity, we also evaluate the semantic room categories predicted by GPT-3.5. Even though MoMa-LLM uses open-set room categories as described in the main manuscript, we evaluate the performance on closed-set room category prediction to allow comparison. To do so, we provided GPT-3.5 with all room categories provided in the iGibson dataset in order to pick the most suitable given the objects assigned to each particular Voronoi component representing a room. Similar to the purity evaluation, we report numbers that are averaged over 10 episodes per scene as well as across all high-level policy steps per episode. We compare the predicted room category of each Voronoi node with the underlying ground-truth room layout maps. Following this, we arrive at an average predicted room category accuracy of 27.6%. The number is further affected by open room layouts as mentioned above.

To provide a comparison, we also evaluated the predicted room categories in an open-set manner on the real-world map

shown in Fig. S.1. Across the 10 trials executed in the real world as given in Tab. III, we follow the same evaluation protocol and obtain an average room category accuracy of 90.1% as listed in Tab. S.2. Human-level assessment allows evaluating errors such as *entryway* instead of *hallway* positively, which drastically increases the metrics. Nonetheless, the real-world map is less complex in terms of topology and object distribution compared to the iGibson environments, which feature, e.g., rooms with no objects contained.

## B. Reasoning

Fig. S.3 shows additional examples of the scene representations and the model reasoning. It depicts the Voronoi graph and frontiers to unexplored areas (left), the BEV-map together with the constructed scene graph (middle), and the input prompt and answers of the LLM (right). Additional video material with full prompt reasoning is shown on the project website.

## REFERENCES

- [1] N. Reimers and I. Gurevych, “Sentence-BERT: Sentence embeddings using Siamese BERT-networks,” in *Proc. of the Conference on Empirical Methods in Natural Language Processing and the International Joint Conference on Natural Language Processing (EMNLP-IJCNLP)*, Nov. 2019, pp. 3982–3992.

- [2] M. Shridhar, J. Thomason, D. Gordon, Y. Bisk, W. Han, R. Mottaghi, L. Zettlemoyer, and D. Fox, “Alfred: A benchmark for interpreting grounded instructions for everyday tasks,” in *Proc. of the IEEE Conf. on Comp. Vision and Pattern Recognition*, 2020, pp. 10 740–10 749.
- [3] F. Schmalstieg, D. Honerkamp, T. Welschehold, and A. Valada, “Learning hierarchical interactive multi-object search for mobile manipulation,” *IEEE Robotics and Automation Letters*, 2023.
- [4] D. Honerkamp, T. Welschehold, and A. Valada, “ $N^2m^2$ : Learning navigation for arbitrary mobile manipulation motions in unseen and dynamic environments,” *IEEE Transactions on Robotics*, 2023.
- [5] G. Chalvatzaki, A. Younes, D. Nandha, A. T. Le, L. F. Ribeiro, and I. Gurevych, “Learning to reason over scene graphs: a case study of finetuning gpt-2 into a robot language model for grounded task planning,” *Frontiers in Robotics and AI*, vol. 10, 2023.